Visualization and Morphological Analysis of Individual Oligodendrocytes in the Mouse White Matter

Yasuyuki Osanai[1,2,5], Sasikarn Looprasertkul[1,3,5], Batpurev Battulga[1], Reiji Yamazaki[1], Nobuhiko Ohno[1,4].

[1.]Department of Anatomy, Division of Histology and Cell Biology, School of Medicine, Jichi Medical University, Shimotsuke, 329-0498, Japan. [2.]Australian Regenerative Medicine Institute, 15 Innovation Walk, Monash University, Clayton, Victoria, 3800, Australia. [3]Section of Electron Microscopy, Supportive Center for Brain Research, National Institute for Physiological Sciences, Okazaki, Japan. [4.]Division of Ultrastructural Research, National Institute for Physiological Sciences, Okazaki, Japan. [5.]These authors contribute equally.

Correspondence:

Yasuyuki Osanai, yasuyuki.osanai@jichi.ac.jp

Abstract

Myelin formation by oligodendrocytes is essential for the regulation of the conduction velocity

and proper brain function. To ensure accurate information processing in response to experiences such as sensory stimuli and learning, oligodendrocytes adjust their number and morphology. In addition, oligodendrocyte morphology changes with senescence and in the presence of neurodegenerative diseases. Thus, visualizing oligodendrocytes and analyzing their morphology is crucial for understanding how our brains change under such conditions. Herein, we describe the methods for labeling and analyzing the morphologies of individual oligodendrocytes in mouse white matter at the light microscopic level. PDGFRa-CreERT2:Tau-mGFP and PLP-CreERT2:Tau-mGFP mice enable us to visualize and analyze later-born or early-born oligodendrocyte morphology. In addition, sparse oligodendrocyte labeling with attenuated rabies virus expressing GFP enables the visualization and morphological analysis of individual oligodendrocytes in various brain white matter regions without the need for transgenic animals. Furthermore, the combination with immunostaining in thick tissues enables the identification of labeled oligodendrocytes and myelin sheaths, as well as their interactions with neuronal axons. These methods are suitable for revealing how oligodendrocytes adapt their morphologies depending on environmental stimuli or pathological conditions.

Keywords

oligodendrocyte, myelination, rabies virus, tissue clearing

Running head

Visualization and analysis of a single oligodendrocyte

1. Introduction

Oligodendrocytes, the myelin sheath-forming glial cells in the central nervous system, are critical for proper brain functions as they regulate the conduction velocity through myelin sheath formation and saltatory conduction and support neuronal metabolism. Physiological and pathological changes in brain functions are often accompanied by the structural regulation of oligodendrocytes and their myelin, which in turn modulates signal transduction in the neural circuits. Neuronal axons can be divided into multiple segments, including internode covered by myelin sheaths and nodes of Ranvier. The nodes of Ranvier are flanked by paranodes involving paranodal loops and axon-oligodendrocyte junctions [1]. Internodes are characterized by multilamellar compact myelin and inner and outer tongue cytoplasmic channels. Each oligodendrocyte, typically with a small cell body, extends multiple processes, with each connected to the outer tongue [2]. Characteristic oligodendrocyte morphology is developed through the differentiation of oligodendrocyte progenitor cells (OPCs), which express markers such as NG2 and PDGFRa and exhibit bipolar shapes, into mature myelinating oligodendrocytes,

55 which test positive for markers such as proteolipid protein (PLP) and myelin basic protein, extend
56 multiple processes, and form myelin sheaths.

57 Compared to other glial cells such as astrocytes and microglia, visualization of
58 oligodendrocytes is difficult because there are no reliable anti-bodies that label both their cell
59 bodies and processes (including myelin). Historically, silver carbonate methods or single-cell
60 injection of lucifer yellow have been used for visualizing the morphology of a single
61 oligodendrocyte [3, 4]. However, as silver carbonate staining requires special fixation and single-
62 cell lucifer yellow injection is technically difficult and makes it hard to obtain high sample
63 numbers, recent studies have focused on the use of transgenic animals and viral vectors [5-7].

64 PDGFRa-CreERT2:Tau-mGFP and PLP-CreERT:Tau-mGFP mice are transgenic lines
65 that label oligodendrocytes differentiated after tamoxifen administration or those generated before
66 tamoxifen administration, respectively [8, 9]. The PDGFRa-CreERT2 mouse expresses
67 tamoxifen-inducible Cre in OPCs, and the Tau-mGFP mouse possess the lox-STOP-lox
68 membrane-targeted GFP (mGFP) cassette downstream of the Tau (MAPT) promoter that is active
69 in neurons and mature oligodendrocytes. Tamoxifen-induced recombination removes the lox-
70 STOP-lox cassette from OPCs, and as they differentiate into oligodendrocytes, GFP expression
71 is driven by the Tau promoter. Thus, in PDGFRa-CreERT2:Tau-mGFP mice, we can label the
72 oligodendrocytes differentiated after the tamoxifen injection. In contrast, in PLP-CreERT mice,

73 tamoxifen-inducible Cre is expressed only in mature oligodendrocytes, since the PLP promoter is
74 active in mature oligodendrocytes but not in OPCs. Therefore, PLP-CreERT:Tau-mGFP mice
75 enable the labeling of oligodendrocytes differentiated before the tamoxifen injection. Thus, in
76 PLP-CreERT:Tau-mGFP mice, we can label early-born oligodendrocytes when we administer
77 tamoxifen in the early developmental period [9]. Therefore, these transgenic animals enable the
78 visualization of a temporarily distinct oligodendrocyte population.

79 Rabies virus and Semliki Forest virus vectors have been used to sparsely label
80 oligodendrocytes in the mouse white matter [10, 11]. We have previously analyzed the
81 interactions between oligodendrocytes and other cells, such as neurons, using a rabies virus vector
82 and immunostaining for thick (> 70μm) sections. Using this method, both single oligodendrocytes
83 and their myelinated axons can be labeled [9]. Thus, it is a powerful tool to analyze
84 oligodendrocyte-neuron interactions.

85 In this paper, we introduce methods to visualize and analyze single-cell oligodendrocyte
86 morphology at the light microscopic level, focusing on two labeling methods employing
87 transgenic mice and a viral vector. The methods using PDGFRa-CreERT2:Tau-mGFP and PLP-
88 CreERT:Tau-mGFP have been validated in the corpus callosum and cerebellum [9, 12], and
89 labeling using the rabies virus vector has been employed in multiple white matter regions,
90 including the corpus callosum, cerebellum, optic nerve and chiasm, and spinal cord [10]. Methods

91 utilizing these transgenic animals are potentially applicable to all brain regions, including the gray
92 matter. The rabies virus-mediated method is considered applicable not only to the white matter of
93 mice but also to that of other animals. These methods can be useful in examining various
94 morphological aspects of individual oligodendrocytes, such as the number of myelin sheaths, the
95 length and fiber diameter of each myelin sheath, height of each oligodendrocyte, and myelination
96 toward a particular subtype of axons.
97
98 **2. Materials**
99
100 **2.1 Transgenic mice and reagents**
101 1. PDGFRa-CreERT2 [13] or NG2-CreERT2 mice (Jackson, strain name: B6.Cg-Tg(Cspg4-
102 cre/Esr1*)BAkik/J, # 008538) [14].
103 2. PLP-CreERT mice (Jackson, strain name: B6.Cg-Tg(Plp1-cre/ERT)3Pop/J, # 005975) [15].
104 3. Tau-mGFP mice (Jackson, strain name: B6;129P2-Mapttm2Arbr/J, # 021162) [16].
105 4. Tamoxifen.
106 5. Corn oil.
107 6. Disposable syringes for small-volume injection.
108 7. 25G short length needles (10–16 mm).

109

110 **2.2 Viral vector and stereotaxic injection**

111 1. Rabies B19G-SADΔG-GFP (Salk Institute, viral vector core) or Rabies B19G-HepΔG-GFP

112 [17] (*See* Note 1 for information on virus production and purchasing).

113 2. Apparatus for stereotaxic microinjection (For detailed procedures of mouse brain stereotaxic

114 injection, please consult methodological papers on viral injection, such as Cetin et al., 2006) [18].

115

116 **2.3 Perfusion and slicing of the brain**

117 1. 4% paraformaldehyde (PFA) in 0.1 M phosphate buffer (PB) (pH 7.4).

118 2. Vibratome slicer.

119 3. Perfusion pump.

120

121 **2.4 Thick tissue immunostaining and tissue clearing with RapiClear**

122 Stock solutions without normal goat serum (NGS) or antibodies can be stored at room temperature

123 (RT; 20–25°C) for over 1 year.

124 1. Penetration buffer: 2% Triton X-100 and 0.05% sodium azide in phosphate-buffered saline

125 (PBS). Mix 2 g of Triton X-100 and 50 mg of sodium azide in 98 mL of PBS.

126 2. Blocking buffer: 10% NGS, 1% Triton X-100, 2.5% dimethyl sulfoxide (DMSO), and 0.1%

127 sodium azide in PBS. Mix 1 g of Triton X-100, and 2.5 g of DMSO in 87 mL of PBS. Add NGS

128 at one-tenth of the final volume to the solution before use.

129 3. Antibody dilution buffer: 1% NGS, 0.2% Triton X-100, 2.5% DMSO and 0.1% sodium azide

130 in PBS. Mix 2 mL of 10% Triton X-100 solution, 2.5 g DMSO, and 100 mg sodium azide in 96

131 mL of PBS. Add NGS at 1/100 of the final volume of the solution immediately before use.

132 4. Washing buffer: 3% NaCl and 0.2% Triton X-100 in PBS. Mix 3 g of NaCl, and 2 mL of 10%

133 Triton X-100 solution in 95 mL of PBS.

134 5. Antibodies: Mouse monoclonal anti-APC (CC1, 1/100, IgG2b, OP80, Merck) for labeling

135 mature oligodendrocytes, rabbit polyclonal anti-human Olig2 (1/100, 18953, Immuno-Biological

136 Laboratories America) or chicken polyclonal anti-Olig2 (1/500, OLIG2-0020, Aves) for labeling

137 oligodendrocyte lineage cells, rabbit polyclonal anti-Iba1 (1/400, 019-19741, Wako) for labeling

138 microglia, mouse monoclonal anti-GFAP (1/100, IgG1, G3893, Sigma-Aldrich) or mouse

139 polyclonal anti-S100B (1/100, ab34686, Abcam) for labeling astrocytes (*see* Note 2), rabbit

140 polyclonal anti-Caspr (1/500-1000, ab34151, Abcam) for labeling the paranodes of the myelin

141 sheath, rabbit polyclonal anti-NG2 (1/50, AB5320, Merck) for labeling OPCs, rabbit polyclonal

142 anti-calbindin (1/500, MSFR100390, Frontier Institute) for labeling Purkinje cells, chicken

143 polyclonal anti-neurofilament-H (1/500, NB300-217, Novusbio) for labeling neuronal axons, and

144 rat monoclonal anti-GFP (1/500, IgG2a, 04404-84, Nacalai Tesuque) for visualizing GFP.

145 6. RapiClear 1.52 (RC152001, SUNJin Lab, Taiwan)

146 7. Antifadant

147

148 **3. Methods**

149

150 **3.1 Labeling oligodendrocytes using PDGFRa-CreERT2:Tau-mGFP and PLP-Cre:Tau-**

151 **mGFP mice**

152 **3.1.1 Tamoxifen administration and fixation**

153 1. PDGFRa-CreERT2 and PLP-CreERT mice are crossed with Tau-mGFP mice to generate

154 PDGFRa-CreERT2 (either homozygous or heterozygous):Tau-mGFP (heterozygous) and

155 PLP-CreERT (either homozygous or heterozygous):Tau-mGFP (heterozygous) mice,

156 respectively.

157 2. Tamoxifen is dissolved in corn oil for one 1 h to make a tamoxifen stock solution (10 mg/mL).

158 During this process, the solution is incubated at 60 °C and vortexed every 10 min. Tamoxifen

159 stock solution can be aliquoted (0.5–1.5 mL) and stored for at least six months at −20°C. The

160 frozen stock solution is incubated at 60°C for 1 h before use, with gentle mixing by vortex

161 every 10 min during incubation. The thawed solution can be stored at 4°C for up to one week.

162 Before injection, the solution is incubated at 60°C for 10 min and vortexed thoroughly.

163 Ideally, the temperature of the solution be 37°C at the time of injection.

164 3. Tamoxifen is administered via intraperitoneal injection (50–100mg/kg) for two consecutive
165 days in mice younger than postnatal day 15 (P15). For mice older than P15, intraperitoneal
166 administration of 100 mg/kg tamoxifen for four consecutive days is recommended (*see* Notes
167 3, 4, and 5).

168 4. Mice are perfused with 4% PFA in 0.1 M PB at the desired postnatal age. Their brains are
169 then postfixed in the same fixative for 1 day at 4°C. After transferring the brains into PBS,
170 100 μm-thick brain slices are prepared using a vibratome slicer (*see* Note 6).

171

172 **3.2 Labeling oligodendrocytes using attenuated rabies virus-GFP**

173 The methods for stereotaxic microinjections are well established; therefore, they are not
174 described in detail here. For the detailed procedure, please refer to methodological papers on
175 stereotaxic injection, such as Cetin et al (2006).

176 1. Dilute the rabies virus stock with PBS to prepare a viral solution containing 5.0×10^3–5.0
177 $\times 10^4$ infectious units per microliter.

178 2. Inject 1 μL of the viral solution into the white matter. The following parameters are used
179 for injections into each brain region. In the adult mouse, for the corpus callosum 1.0 mm
180 posterior and 0.5–0.8 mm lateral to the bregma, at a depth of 1.0 mm from the pia, for the

181 optic chiasm, 0.2 mm posterior and 0.0 mm lateral to the bregma, at a depth of 5.0–5.3
182 mm from the pia, and for the white matter of cerebellar lobules IV/V, 6.45 mm posterior
183 and 1.00 mm lateral to the bregma, a depth of 0.5 mm.

184 3. Perfuse mice with 4% PFA in 0.1 M PB, 4–7 days after viral injection. The brains are then
185 postfixed in the same fixative for 1 day at 4°C. After transferring the brains into PBS, 100
186 μm-thick brain slices are prepared using a vibratome slicer.

187

188 **3.3 Immunostaining of thick brain sections using the Rapi clear method to analyze**
189 **oligodendrocyte morphology**

190 1. Select brain sections (50–200 μm) containing the target brain region and place 2–3
191 sections per well into a 24-well plate filled with PBS.

192 2. Incubate brain sections in the penetration buffer at RT for 24 h.

193 3. Incubate the brain sections in the blocking buffer for 1–2 days at 4°C,

194 4. The sections are incubated at 4°C for 3–4 days in the antibody dilution buffer (300-500
195 μL for 2–3 sections in 24 well plate) containing primary antibodies such as rat anti-GFP
196 (1/500), rabbit anti-Caspr (1/500-1000), rabbit anti-human Olig2 (1/100) or chicken anti-
197 Olig2 (1/500), and mouse anti-APC (CC1, 1/100).

198 5. Wash the sections in washing buffer three times for 1 h each at RT. Then, incubate the

199 specimens in washing buffer on an orbital shaker at 4°C overnight.

200 6. Incubate the specimens with secondary antibodies in the antibody dilution buffer on an
201 orbital shaker at 4°C for 2 days.

202 7. Wash the sections in washing buffer three times for 1 h each at RT. Then, keep the
203 specimens in the washing buffer on an orbital shaker at 4°C overnight.

204 8. Stain with Hoechst (1/1500–2000) in PBS for 3 h at RT if needed.

205 9. If the tissue was stained with Hoechst, wash it with PBS three times for 1 h each on an
206 orbital shaker at RT. If not, with PBS twice for 10 min each.

207 10. For tissue clearing, place the specimen on a slide glass, add pre-warmed (37°C) RapiClear
208 solution with/without an antifade solution. After 20 min, applying the cover glass.

209 11. Apply the cover glass and seal its edges with a clear nail polish. Allow the slide to dry
210 overnight at RT (*see* Note 7).

211

212 **3.4. Confocal microscopic imaging**

213 Use a confocal microscope with Z-series sequential imaging function. A single
214 oligodendrocyte morphology can be captured by approximately 50–100 optical sections at 0.5
215 μm intervals, adjusted as needed to fully capture the dorsal-ventral extent of the cell bodies,
216 processes, and myelin sheaths of individual oligodendrocytes. We utilized a 60× objective lens

217 (N.A. 1.42) on the Dragonfly 200 high-speed confocal platform to achieve the high–
218 magnification image. High–resolution images are required for detailed morphological analyses
219 of individual oligodendrocytes and their myelin internodes.
220
221 1. The uppermost and lowermost individual oligodendrocytes and their myelin are set for
222 image acquisition, with a step size of 0.5 μm. GFP signal loss is used to define the
223 uppermost and lowermost limits of the confocal Z-stack imaging.
224 2. Images are captured and exported in the proprietary file format provided by the microscope
225 manufacturer. The subsequent analysis is performed using the Fiji software, which supports
226 most proprietary formats, such as .oif, .nd2, .czi, and .ims. These formats preserve z-plane
227 and scale information, facilitating the analysis of entire individual oligodendrocytes with
228 Fiji.
229
230 **3.5. Analysis of oligodendrocyte morphology labeled using PDGFRa-CreERT2:Tau-mGFP**
231 **and PLP-Cre:Tau-mGFP mice**
232 The oligodendrocyte in PDGFRa-CreERT2:Tau-mGFP (Fig. 1) and PLP-Cre:Tau-
233 mGFP mice (Fig. 2) are labeled via tamoxifen-induced Cre recombination at specific time points.
234 The oligodendrocyte cell membrane and myelin sheath membrane can be labeled by mGFP,

235 which enables the analysis of the oligodendrocyte's morphology. The age of mice, number of
236 administrations, and concentration of the tamoxifen are important for the analysis of a single
237 oligodendrocyte. If oligodendrocytes are densely labeled, it becomes difficult to analyze the
238 morphology of individual cells. Various morphological aspects can be analyzed in single
239 oligodendrocytes (*see* Note 8), such as the myelin sheath length, number of myelin sheaths
240 produced by a single oligodendrocyte [8, 19], fiber diameter of each myelin sheath [20], and
241 heights of single oligodendrocytes [12].
242
243 **3.5.1 Measurement of the length and number of myelin sheaths formed by a single**
244 **oligodendrocyte**
245 1. The number of sheaths and the myelin sheath length produced by a single oligodendrocyte
246 are quantified using the Simple Neurite Tracer (SNT) plugin
247 (https://imagej.net/plugins/snt/) [21], accessed via Fiji via Plugins > Neuroanatomy >
248 SNT....
249 2. In the SNT Startup Prompt window, select the directory containing the target file that
250 includes the z-stacked serial images of the GFP-labeled oligodendrocyte and its myelin
251 sheaths.
252 3. Since the images may appear with low intensity, adjust the brightness and contrast as needed

253 via Fiji > Image > Adjust > Brightness/Contrast….

254 4. Each individual myelin sheath is manually traced in the z-stacked serial images. The starting
255 point of each myelin sheath is defined at one tip of the myelin sheath (GFP-positive)
256 colocalized with the paranode marker (Caspr-positive, Fig. 1g–i), and subsequent points are
257 selected along the trajectory of the sheath across adjacent optical sections. Press either "Yes"
258 or the "Y" key to accept the path. For each pair of selected points, the A* search path-
259 finding algorithm auto-tracing within SNT is used to compute the optimal path based on
260 image intensity gradients. Each path segment is accepted by pressing the "Y" key. After
261 completing a full trace of one sheath, the path is finalized by selecting "Finish" or pressing
262 the "F" key.

263 5. Each completed myelin sheath tracing is stored as an individual path and can be verified
264 using SNT Path Manager (Fig. 1k, l).

265 6. After tracing all the myelin sheaths of a single oligodendrocyte, save the tracing data as
266 follows: File > Save Tracings… > Save As… (.traces file).

267 7. To determine the length of each myelin sheath and the total number of sheaths per cell,
268 export the path statistics via Analysis > Path Properties: Export CSV….

269

270 **3.5.2 Height/ vertical territory measurement of an individual oligodendrocyte**

1. Acquire z-stacked serial images of individual oligodendrocytes at a 0.5 μm step size, ensuring that all myelin sheaths of the cell are included. Images should be saved in a file format compatible with the Fiji software.
2. Import the z-stacked serial images into the Fiji software. The imported images display the entire oligodendrocyte, with all its myelin sheaths.
3. Since the images may appear with low intensity, adjust the brightness and contrast appropriate via Fiji > Image > Adjust > Brightness/Contrast….
4. Identify the outermost dorsal and ventral myelin processes of the oligodendrocyte using the z-stack images.
5. Locate the uppermost dorsal and lowermost ventral myelin sheaths by tracing along their full length and identifying the connection point between each myelin sheath and the corresponding oligodendrocyte process.
6. Mark these connection points for further analysis.
7. Locate and mark the nucleus of each individual oligodendrocyte in the z-stack images.
8. Compress the confocal z-stack into a single-plane projection for linear distance measurement via Image > Stacks > Z Project...
9. Measure the distance between the points where the outermost dorsal and ventral myelin internodes connect to their process by drawing a straight line from the dorsal outermost

289 myelin sheath to the ventral outermost one. Ensure that the line passes through the nucleus
290 and is perpendicular to the connection points of the processes (Fig. 1j). This can be done
291 via Analyze > Measure.

292 **3.5.3 Fiber diameter measurement of a single oligodendrocyte**

293 1. Acquire z-stacked serial images of individual oligodendrocytes at a 0.5 μm step size,
294 ensuring the inclusion of all myelin sheaths of the cell. Images should be saved in a file
295 format compatible with the Fiji software.
296 2. Import the z-stacked serial images into the Fiji software. The imported images display the
297 entire oligodendrocyte, including all its myelin sheaths.
298 3. Since the images may appear with low intensity, adjust the brightness and contrast
299 appropriate via Fiji > Image > Adjust > Brightness/Contrast….
300 4. Select the myelin sheaths of each oligodendrocyte to measure their diameters. One approach
301 is to include: (i) the outermost myelin sheath on the dorsal side, (ii) the outermost sheath
302 on the ventral side, (iii) one internode located in the central region of the oligodendrocyte,
303 (iv) one internode between the central region and the outermost dorsal sheath, and (v) one
304 internode between the central region and the outermost ventral sheath, based on z-stack
305 images.
306 5. Compress the Z-stacked image to a single plane image. To determine where to measure the

307 diameter, draw a line parallel to the myelin internode of the selected myelin sheath and
308 measure the length of that line (Fig. 1m).
309 6. Since the fiber diameters can vary along the internode, myelin internodes are divided into
310 several segments for measurement. For example, the internodes are divided into six
311 segments using the following formula to determine the spacing along their total length:
312 Distance for measurement position (μm) = (Internode length (μm) − 2 μm) / 5
313 Place the first and last measurement points at a distance of 1 μm from each end of the
314 myelin internode because the internode's tip is a paranode area that is always larger than
315 the internode. The remaining four points are positioned equally between them based on
316 the calculated distance.
317 7. After the positions for the measurement are marked (Fig. 1m), draw a line from the upper
318 part to the lower part of that myelin area and measure its length (Fig. 1n) via Analyze >
319 Measure.
320 8. Collect data on the selected positions of each myelin sheath and calculate the average fiber
321 diameter.
322 9. Measure the fiber diameter of the selected internodes per oligodendrocyte—approximately
323 five internodes per oligodendrocyte. Then, calculate the average fiber diameter of each
324 oligodendrocyte.

325

326 **3.6 Analysis of selective myelination toward a particular subtype of axons**

327 We have previously demonstrated that oligodendrocytes that differentiated early in life
328 preferentially myelinate Purkinje cell axons in the cerebellar white matter [9]. By combining the
329 RapiClear method with oligodendrocyte labeling using transgenic mice or rabies virus, we are
330 able to investigate the selective myelination toward specific axon subtypes.

331

332 1. Label oligodendrocytes using transgenic mice or rabies virus. We labeled early-born
333 oligodendrocytes in PLP-CreERT:Tau-mGFP mice by administering tamoxifen at P8 (100
334 mg/kg) and perfusing the animals with 4% PFA in 0.1 M PB at P56 (Fig. 2).
335 2. Prepare 100 μm brain slices using a vibratome.
336 3. Performing thick-section immunostaining, RapiClear method, as described above, using
337 markers for specific neuronal subtypes (e.g., calbindin for Purkinje cell axons) and the
338 pan-neuronal axon marker neurofilament. GFP-labeled oligodendrocytes in transgenic
339 animals should be enhanced with an anti-GFP antibody, whereas those labeled by rabies
340 virus do not require immunostaining.
341 4. Acquire z-series confocal images of GFP-labeled oligodendrocyte/myelin and multiple
342 subtypes of neuronal axons as described above.

343 5. Count the number of axons of each subtype myelinated by the GFP-labeled sheath using
344 Fiji. GFP-labeled processes ensheathing axons for more than 20 μm were defined as
345 myelin sheaths (*see* note 9).
346 6. Count the number of axons of each subtype not myelinated by GFP-labeled
347 oligodendrocyte/myelin within the height of the labeled oligodendrocytes (Fig. 2).
348 7. To determine whether GFP-labeled oligodendrocytes preferentially myelinate specific axon
349 subtypes, perform Fisher's exact test for individual confocal images using statistical
350 software (e.g., Prism, GraphPad). Input the following values:
351 A. Number of specific-subtype axons myelinated by GFP-labeled oligodendrocytes,
352 B. Number of specific-subtype axons not myelinated,
353 C. Number of non-specific-subtype axons myelinated,
354 D. Number of non-specific-subtype axons not myelinated.
355 Fisher's exact test is then performed to evaluate selective myelination.
356

357 **3.7 Analysis of single oligodendrocytes morphology labeled by attenuated rabies virus**

358 While the morphological analyses of individual oligodendrocytes in the sections labeled
359 with the rabies virus are mostly similar to those in PDGFRa-CreERT2:Tau-mGFP and PLP-
360 CreERT:Tau-mGFP mice, there are some differences. The GFP expression level in cells infected

361 by attenuated rabies virus encoding GFP (hereafter referred to as RV-GFP) is so strong that
362 immunostaining for GFP is unnecessary. Since RV-GFP can label cells other than
363 oligodendrocyte-lineage cells, we first need to check whether the cells labeled with RV-GFP are
364 oligodendrocytes. If the labeled cells exhibit morphological features of myelinating mature
365 oligodendrocytes and have GFP-positive ensheathment around neuronal axons, which are mostly
366 flanked by Caspr immunostaining, these cells are identified as oligodendrocytes.

367 In the white matter, myelinating mature oligodendrocytes labeled with RV-GFP extend
368 the processes corresponding to their myelin sheaths parallel to the direction of the neuronal axons.
369 Because RV-GFP labels the cytosol of myelin sheaths, the ensheathment of the GFP signal around
370 unstained axons can be clearly observed when the diameters of these axons are large (Fig. 3a, *see*
371 Note 9). Another distinguishing feature of RV-GFP-labeled oligodendrocytes is the swelling
372 observed at the paranodal regions (Fig. 3). Since the paranodes contain more cytoplasm than the
373 internodes, the paranodes appear more intensely labeled and expanded with GFP. The length of
374 each myelin sheath can be measured by identifying its paranodes as GFP-labeled swellings at
375 both ends of the sheath.

376 We can also use antibodies against oligodendrocytes/myelin markers. Notably, cell
377 body markers for oligodendrocytes (e.g., CC1) tend to be downregulated in RV-GFP (+) cells,
378 which might be attributed to the high-level GFP expression. To confirm whether GFP-labeled

379 cells form the myelin sheath, we recommend using an anti-Caspr antibody. If the ends of GFP-
380 positive processes are closely aligned with Caspr signals, this indicates that the processes
381 correspond to the myelin sheath flanked by the set of Caspr signals (Fig. 3). These morphological
382 features, combined with immunostaining, allow for reliable oligodendrocyte identification.
383

384 **4. Notes**

385 1. Salk Institute viral vector core provides a stock G-deleted rabies aliquot. Rabies virus vector
386 amplification techniques have been described in several studies [22, 23]. Rabies B19G-SADΔG-
387 GFP and rabies B19G-HepΔG viral vectors can be obtained from Vector Builder (Chicago, USA).
388

389 2. Immunostaining of membrane-located receptors is not always successful for the thick-tissue
390 immunostaining method. For example, immunostaining for PDGFRa is difficult with this method.
391 If you want to count the number of OPCs, we recommend quantifying CC1(−)/Olig2 cells [24] or
392 using immunostaining for NG2 [12]. In our experience, the anti-GFAP antibody exhibits reliable
393 performance in brain tissue, whereas the anti-S100B antibody lacks astrocyte specificity,
394 particularly in the corpus callosum. In contrast, in the optic nerve, anti-GFAP antibodies are
395 ineffective, but the anti-S100B antibody works well. To accurately determine the number of
396 astrocytes in the optic nerve, double immunostaining with anti-S100B and anti-Olig2 antibodies

397 is recommended, as both astrocytes and OPCs express S100B.

398

399 3. In our experience, 100 mg/kg tamoxifen administration for more than two days increases the

400 risk of mortality in mice younger than P15. Researchers should first confirm whether the mouse

401 strain they are using can tolerate two consecutive days of tamoxifen administration. If the

402 mortality rate is high, the number of tamoxifen administration days or its dosage should be

403 reduced.

404

405 4. In our experience, tamoxifen administration before P9 failed to label oligodendrocytes; instead

406 it labeled unidentified cells in PDGFRa-CreERT2:Tau-mGFP mice, possibly because PDGFRa

407 promoter activity is not yet restricted to OPC at such an early developmental stage.

408

409 5. Four days of consecutive injection of tamoxifen at 100 mg/kg helps maximize the

410 recombination rate. If a lower recombination rate is acceptable or if you wish to limit the number

411 of labeled oligodendrocytes, consider reducing the tamoxifen concentration or the number of

412 injection days. In PLP-CreERT:Tau-mGFP mice, oligodendrocytes in the white matter tend to be

413 densely labeled [9]. Therefore, to achieve sparse labeling and enable observation of single-cell

414 morphology, the tamoxifen concentration must be substantially reduced.

415

416 6. Brain slices can be stored for up to six months at 4°C in PBS containing 0.1% sodium azide or

417 stored for up to two years at −80°C after freezing in PBS containing 30% sucrose. Before freezing,

418 the slices are incubated in PBS containing 30% sucrose overnight. The GFP signal of Tau-mGFP

419 mouse tissue is weak and needs to be enhanced by immunostaining for GFP prior to imaging.

420

421 7. The immunostained sections embedded on slides can be stored at 4°C for up to one month. For

422 longer storage, the slides need to be stored at −20°C.

423

424 8. During the tracing process, it is important to distinguish the GFP-positive myelin sheaths of

425 the target oligodendrocyte from those of neighboring cells. Because adjacent oligodendrocytes

426 can also express GFP, their myelin sheaths may appear to be in close proximity, potentially

427 leading to misidentification. To avoid this issue, for the morphological analysis of single

428 oligodendrocytes, only cells that are isolated within the field of view (regions where a single GFP-

429 positive oligodendrocyte was clearly identifiable) are selected for tracing. Furthermore, only

430 myelin sheaths directly connected to the cell body through proximal processes of the targeted

431 oligodendrocyte are included in the analysis.

432

433 9. Myelination analyses performed on large-caliber axons, such as cerebellar white matter and the
434 optic nerve, are easier and more reliable compared to those performed on small-caliber axons,
435 such as the axons in the corpus callosum, because we can clearly observe GFP-positive processes
436 ensheathing neuronal axons (Figs. 2 and 3) [25].
437
438 **References**
439
440 1. Stadelmann C, Timmler S, Barrantes-Freer A and Simons M (2019) Myelin in the Central
441 Nervous System: Structure, Function, and Pathology. Physiol Rev 99(3):1381-1431
442 doi:10.1152/physrev.00031.2018
443 2. Osanai Y, Yamazaki R, Shinohara Y and Ohno N (2022) Heterogeneity and regulation of
444 oligodendrocyte morphology. Front Cell Dev Biol 10:1030486 doi:10.3389/fcell.2022.1030486
445 3. Pérez-Cerdá F, Sánchez-Gómez MV and Matute C (2015) Pío del Río Hortega and the
446 discovery of the oligodendrocytes. Front Neuroanat 9:92 doi:10.3389/fnana.2015.00092
447 4. Weruaga-Prieto E, Eggli P and Celio MR (1996) Topographic variations in rat brain
448 oligodendrocyte morphology elucidated by injection of Lucifer Yellow in fixed tissue slices. J
449 Neurocytol 25(1):19-31 doi:10.1007/bf02284783
450 5. Bacmeister CM et al. (2022) Motor learning drives dynamic patterns of intermittent myelination

451 on learning-activated axons. Nat Neurosci 25(10):1300-1313 doi:10.1038/s41593-022-01169-4

452 6. Osso LA, Rankin KA and Chan JR (2021) Experience-dependent myelination following stress

453 is mediated by the neuropeptide dynorphin. Neuron 109(22):3619-3632.e3615

454 doi:10.1016/j.neuron.2021.08.015

455 7. Summers BS et al. (2025) Demyelination Produces a Shift in the Population of Cortical Neurons

456 That Synapse with Callosal Oligodendrocyte Progenitor Cells. eNeuro 12(6)

457 doi:10.1523/eneuro.0113-25.2025

458 8. Young KM et al. (2013) Oligodendrocyte dynamics in the healthy adult CNS: evidence for

459 myelin remodeling. Neuron 77(5):873-885 doi:10.1016/j.neuron.2013.01.006

460 9. Battulga B et al. (2025) Axonal Selectivity of Myelination by Single Oligodendrocytes

461 Established During Development in Mouse Cerebellar White Matter. Glia 73(4):873-886

462 doi:10.1002/glia.24660

463 10. Osanai Y et al. (2017) Rabies virus-mediated oligodendrocyte labeling reveals a single

464 oligodendrocyte myelinates axons from distinct brain regions. Glia 65(1):93-105

465 doi:10.1002/glia.23076

466 11. Toth E, Rassul SM, Berry M and Fulton D (2021) A morphological analysis of activity-

467 dependent myelination and myelin injury in transitional oligodendrocytes. Sci Rep 11(1):9588

468 doi:10.1038/s41598-021-88887-0

469 12. Looprasertkul S, Yamazaki R, Osanai Y and Ohno N (2025) Reduced Accumulation Rate and
470 Morphological Changes of Newly Generated Myelinating Oligodendrocytes in the Corpus
471 Callosum of Aged Mice. Glia 73(11):2322-2334 doi:10.1002/glia.70070
472 13. Rivers LE et al. (2008) PDGFRA/NG2 glia generate myelinating oligodendrocytes and
473 piriform projection neurons in adult mice. Nat Neurosci 11(12):1392-1401 doi:10.1038/nn.2220
474 14. Zhu X et al. (2011) Age-dependent fate and lineage restriction of single NG2 cells.
475 Development 138(4):745-753 doi:10.1242/dev.047951
476 15. Doerflinger NH, Macklin WB and Popko B (2003) Inducible site-specific recombination in
477 myelinating cells. Genesis 35(1):63-72 doi:10.1002/gene.10154
478 16. Hippenmeyer S et al. (2005) A developmental switch in the response of DRG neurons to ETS
479 transcription factor signaling. PLoS Biol 3(5):e159 doi:10.1371/journal.pbio.0030159
480 17. Mori T and Morimoto K (2014) Rabies virus glycoprotein variants display different patterns
481 in rabies monosynaptic tracing. Front Neuroanat 7:47 doi:10.3389/fnana.2013.00047
482 18. Cetin A et al. (2006) Stereotaxic gene delivery in the rodent brain. Nat Protoc 1(6):3166-3173
483 doi:10.1038/nprot.2006.450
484 19. Pitman KA et al. (2020) The voltage-gated calcium channel CaV1.2 promotes adult
485 oligodendrocyte progenitor cell survival in the mouse corpus callosum but not motor cortex. Glia
486 68(2):376-392 doi:10.1002/glia.23723

487 20. Tanaka T et al. (2021) Large-scale electron microscopic volume imaging of interfascicular
488 oligodendrocytes in the mouse corpus callosum. Glia 69(10):2488-2502 doi:10.1002/glia.24055
489 21. Arshadi C et al. (2021) SNT: a unifying toolbox for quantification of neuronal anatomy. Nat
490 Methods 18(4):374-377 doi:10.1038/s41592-021-01105-7
491 22. Wickersham IR, Finke S, Conzelmann KK and Callaway EM (2007) Retrograde neuronal
492 tracing with a deletion-mutant rabies virus. Nat Methods 4(1):47-49 doi:10.1038/nmeth999
493 23. Osakada F and Callaway EM (2013) Design and generation of recombinant rabies virus vectors.
494 Nat Protoc 8(8):1583-1601 doi:10.1038/nprot.2013.094
495 24. Cooper JJM et al. (2023) Chronic demyelination of rabbit lesions is attributable to failed
496 oligodendrocyte progenitor cell repopulation. Glia 71(4):1018-1035 doi:10.1002/glia.24324
497 25. Osanai Y et al. (2018) Length of myelin internodes of individual oligodendrocytes is controlled
498 by microenvironment influenced by normal and input-deprived axonal activities in sensory
499 deprived mouse models. Glia 66(11):2514-2525 doi:10.1002/glia.23502
500
501
502
503 **Figure legends**
504

505 **Fig 1. Visualization and morphological analysis of individual oligodendrocytes in the corpus**

506 **callosum of PDGFRa-CreERT2:Tau-mGFP double transgenic mice.**

507 (a-f) Representative z-stacked images of an oligodendrocyte in the corpus callosum of 10-week-

508 old PDGFRa-CreERT2:Tau-mGFP mice that were injected tamoxifen two weeks before

509 perfusion. The tissue was immunostained for GFP (green), CC1 (white), Caspr (red),

510 counterstained with Hoechst (blue), and imaged using a confocal microscope. The rectangles in

511 the left panels (a–c) are magnified in the right panels (d–f). (g–i) A higher-magnification z-stacked

512 image of the area marked by the rectangle in d. The image shows a GFP-labeled myelin sheath

513 (green, g and i) flanked by Caspr-positive paranodes (red, arrowheads, h and i). This method

514 illustrates a single myelin sheath observable in the z-stacked serial images. (j) GFP-labeled

515 oligodendrocyte (green, arrowhead) in a z-stacked image; double-headed arrow indicates cell

516 height. (k–l) A z-stacked image shown in i with the yellow line added in the analysis with the

517 SNT plugin in Fiji. The GFP-positive myelin sheath (green, k), flanked by Caspr-positive

518 paranodes (red, k), is traced with a yellow line (k and l), representing the path used to measure

519 the length of a single internode formed by an individual oligodendrocyte. This tracing was

520 performed across z-stacked serial images. (m–n) Representative images showing fiber diameter

521 measurement (axonal diameter + myelin thickness) of a single internode shown in g. A GFP-

522 labeled myelin sheath of the individual oligodendrocyte was selected and traced along its full

523 length using a z-stacked serial image. A segmented line was then drawn on a single plane of the
524 z-stacked image and divided into five segments, starting 1 μm from the tip of each side (the white
525 line and its segment lines, m). Fiber diameters were measured at six points along each internode
526 (the arrowheads indicate measurement sites and double-headed arrows indicate span of the fiber
527 diameter, n).
528
529 **Fig 2. Analysis of Purkinje cell selective myelination by early-born oligodendrocytes using**
530 **PLP-CreERT:Tau-mGFP double transgenic mouse.**
531 Representative single-plane confocal image of cerebellar white matter of an 8-week-old PLP-
532 CreERT:Tau-mGFP double transgenic mouse treated with a single tamoxifen injection at P8. (a)
533 GFP-labeled early-born oligodendrocytes and their myelin sheaths (green). (b) Merged image
534 showing Purkinje cell axons (calbindin, red) and early-born oligodendrocytes (GFP, green). (c)
535 Neuronal axons (neurofilament, white), including Purkinje cell axons and other axon subtypes,
536 along with early-born oligodendrocytes (green). (d) Confocal image showing Purkinje cell axons
537 (red), neurofilament-positive axons (white), and early-born oligodendrocytes with their myelin
538 sheaths (green). Due to close proximity of labeled oligodendrocytes, individual cells cannot be
539 clearly distinguished. However, since individual myelin sheath can be identified, we enable to
540 assess whether early-born oligodendrocytes preferentially myelinate Purkinje cell axons (*see* note

541 5).

542

543 **Fig 3. Oligodendrocytes labeled by RV-GFP.**

544 (a–c) RV-GFP-labelled oligodendrocytes in the optic chiasm (a), cerebellar white matter (b), and

545 corpus callosum (c) of 8-week-old mice perfused 4 days after injection. (d–f). Double-

546 fluorescence images of the GFP and Caspr signals in the region outlined by the white square in

547 panels a–c. respectively. The distal ends of processes are co-localized with Caspr signals,

548 indicating that the processes are myelin sheaths.

549

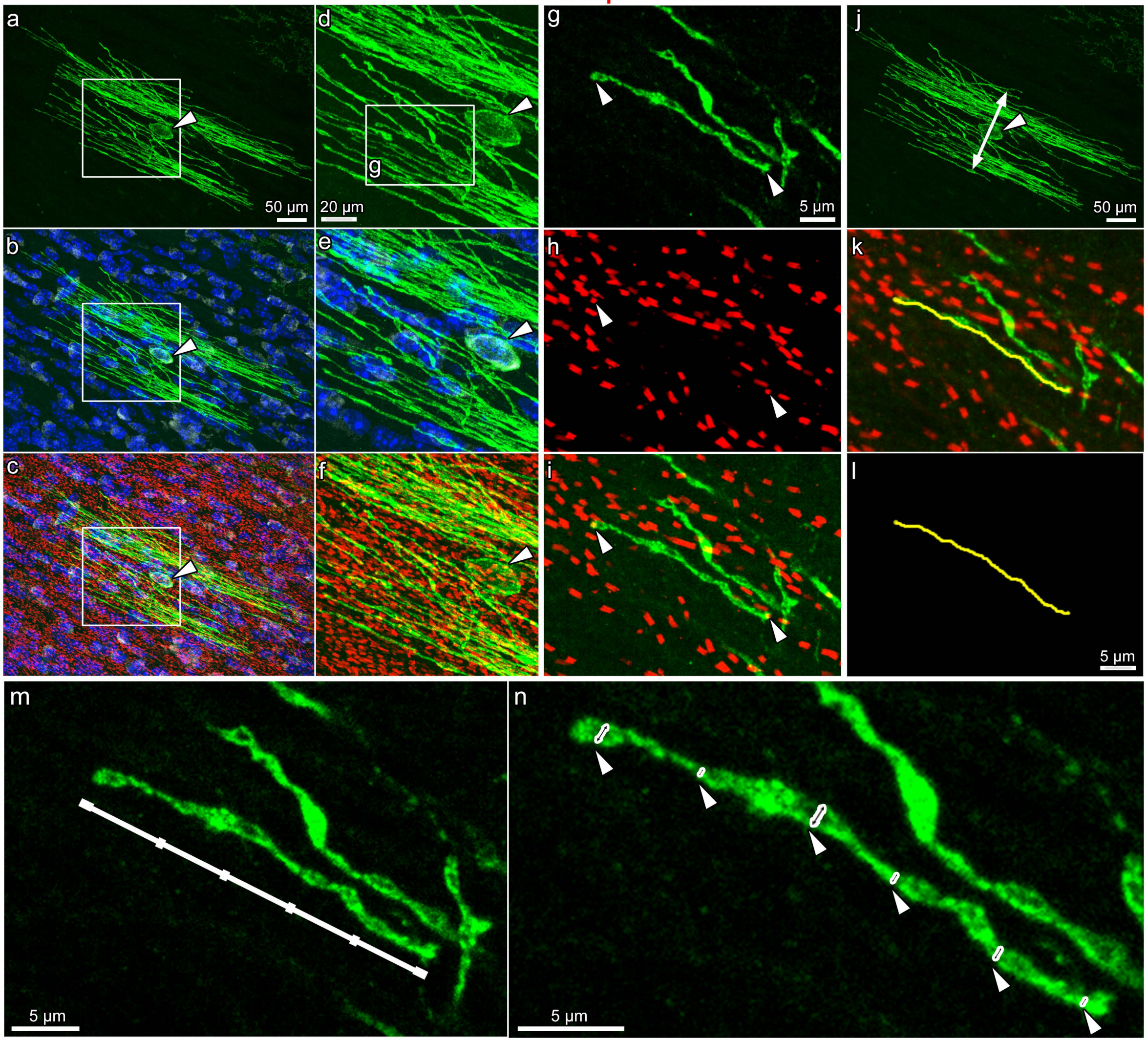
GFP/CC1/Caspr/Hoechst
a
50 µm
d
g
20 µm
g
5 µm
j
50 µm
b
e
h
k
c
f
i
l
5 µm
m
5 µm
n
5 µm

GFP/Calbindin/Neurofilament

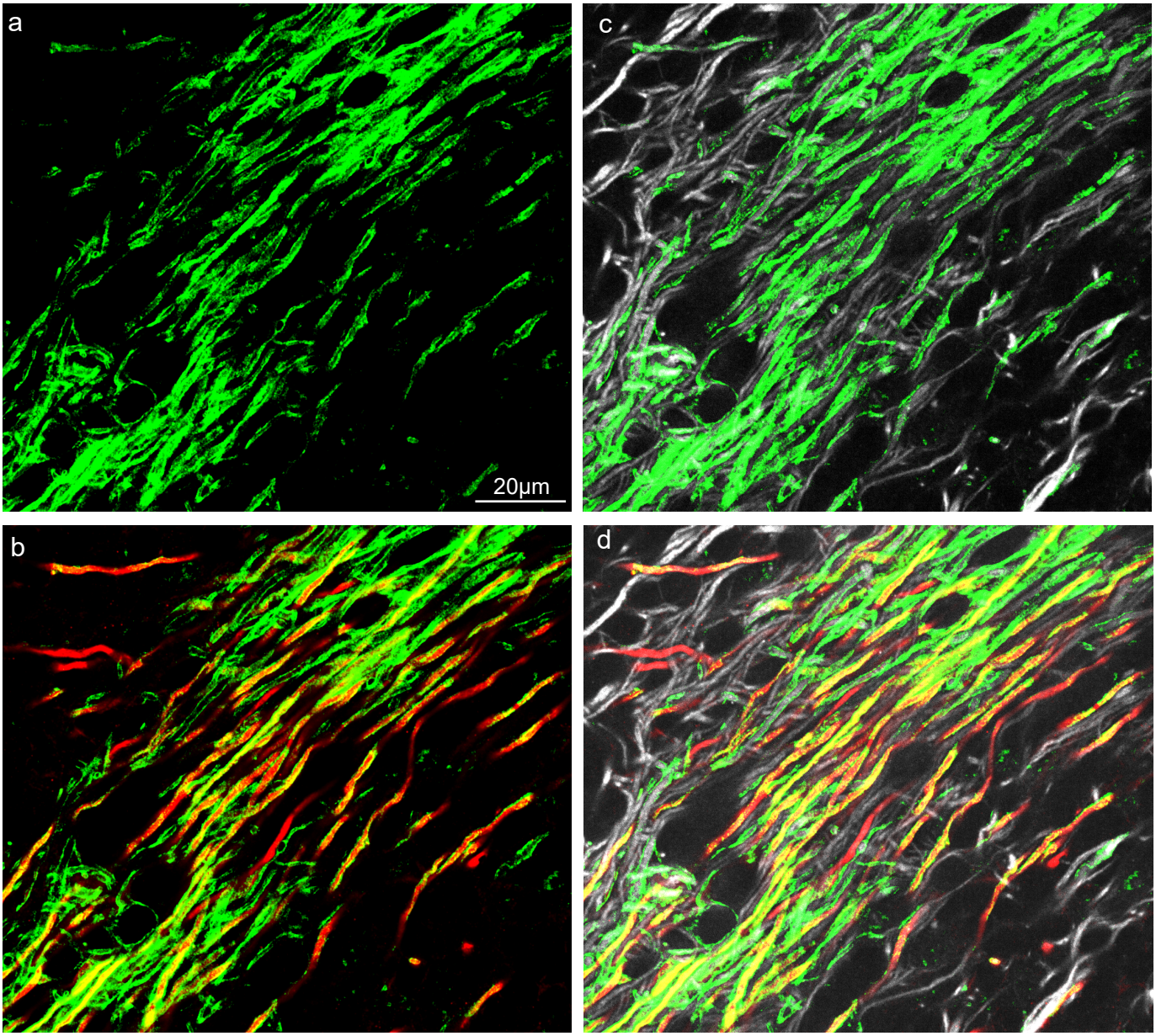

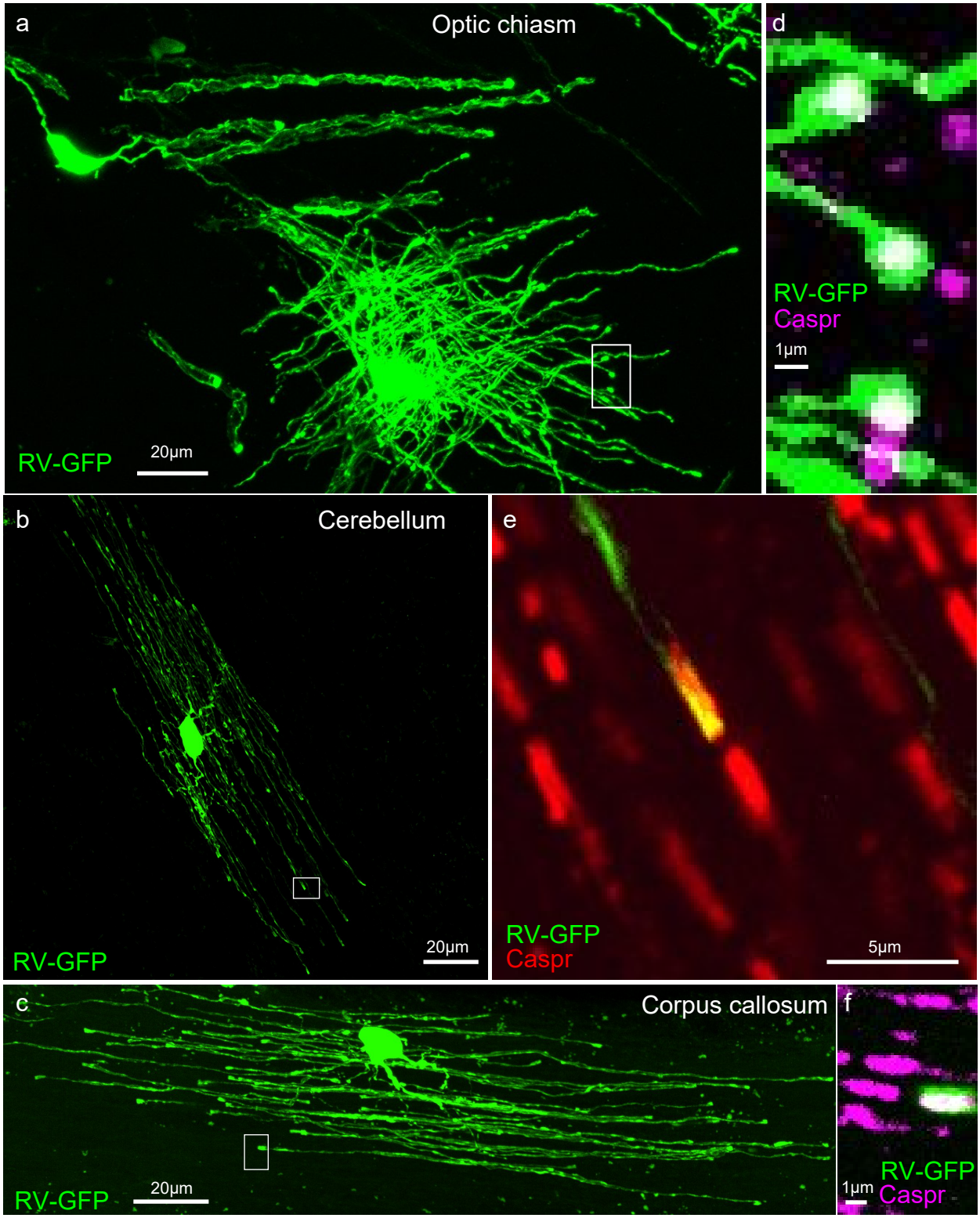
a
Optic chiasm
RV-GFP
20μm
d
RV-GFP
Caspr
1μm
b
Cerebellum
RV-GFP
20μm
e
RV-GFP
Caspr
5μm
c
Corpus callosum
RV-GFP
20μm
f
1μm
RV-GFP
Caspr